J. Phys. B: At. Mol. Opt. Phys. **31** (1998) 2585–2599. Printed in the UK PII: S0953-4075(98)90975-0

Li(2p ← 2s) excitation by impact of slow ions

R Brandenburg†, J Schweinzer‡, F Aumayr† and H P Winter‡§

† Institut für Allgemeine Physik, TU Wien, Association EURATOM-OEAW, A-1040 Wien, Austria

‡ Max-Planck-Institut für Plasmaphysik, EURATOM Association, D-85748 Garching, Germany

Received 23 January 1998, in final form 23 March 1998

Abstract. We present a systematic experimental and theoretical study of Li(2p ← 2s) excitation by impact of slow ($v \leqslant 1$ au) singly and multiply charged ions. In particular, the scaling behaviour of excitation cross sections $\sigma_{\mathrm{Li\,I}}$ with projectile ion charge state q is investigated. Due to the dominance of competing electron capture channels at low impact energies E, the excitation cross sections deviate significantly from a commonly applied $\sigma/q = f(E/q)$ cross section scaling relation.

1. Introduction

Plasma–wall interaction and impurity transport processes in the edge region of magnetically confined fusion plasmas need to be well controlled for successful development of future thermonuclear fusion reactors. An impressive amount of information with excellent spatial and temporal resolution can be obtained from injecting a fast Li atom beam into the plasma edge (Wolfrum *et al* 1993). Li-beam plasma spectroscopy has already become a standard method for reconstructing electron-density profiles from line radiation emitted by collisionally excited Li atoms (Schweinzer *et al* 1992, Aumayr *et al* 1992). In addition, impurity ion concentration and temperature profiles can be obtained from characteristic line emission following electron capture from the injected Li atoms (Schorn *et al* 1991, 1992).

Utilization of these capabilities requires a reliable data base for all relevant collisional processes involving Li atoms and plasma constituents (electrons, hydrogen ions and impurities in different charge states), as well as a precise modelling of the Li beam composition and its attenuation (Wolfrum *et al* 1993, Schweinzer *et al* 1992). Recently, an atomic data base was established which contains relevant evaluated experimental and theoretical cross sections (Wutte *et al* 1997) for collisions of Li atoms with electrons and protons in a wide energy range, regarding the interaction of the injected Li beam with a clean hydrogen plasma.

For accurate evaluation of diagnostic data from the plasma edge, however, also impurity ions have to be taken into account. Regarding collisions of Li atoms with multiply charged ions, only single-electron capture (SEC) has been investigated experimentally and theoretically (Schweinzer *et al* 1994 and references therein), whereas impact excitation has been studied almost exclusively theoretically (Schweinzer *et al* 1992, Ermolaev *et al* 1987), with experimental results so far being only available for impact of He^{2+} on Li (Kadota *et al*

§ Correspondence address: Hannspeter Winter, Institut für Allgemeine Physik, TU–Wien, A-1040 Vienna, Austria. E-mail address: winter@iap.tuwien.ac.at

0953-4075/98/112585+15$19.50

1982). Therefore, more experimental and theoretical information on target excitation (TX) in collisions of slow ($v < 1$ au) multiply charged ions Z^{q+} with Li atoms are of interest.

For TX of Na atoms there is no general scaling relation at low impact energies (Horvath *et al* 1996). Scaling of reduced cross sections σ/q with reduced impact energies E/q (Janev and Presnyakov 1980) is restricted to impact energies $E/q > 15$ keV amu^{-1}. A recent more general scaling (Janev 1996) for $E/q > 25$ keV amu^{-1} concerning dipole-allowed as well as dipole-forbidden excitation gives non-scaled excitation cross sections for fixed E which do not saturate towards high q values but rather decrease beyond a maximum obtained for certain q.

This work, as a combined experimental and theoretical study, focuses on TX of Li(2s) atoms by impact of various slow Z^{q+} ions ($E \leqslant 25$ keV amu^{-1}). Experimental investigations of the collision systems $[Z^{q+}] + \mathrm{Li(2s)} \rightarrow [Z^{q+}] + \mathrm{Li^*(2p)}$ with $Z^{q+} = \mathrm{He^{2+}}, \mathrm{C^{2+}}, \mathrm{C^{4+}}, \mathrm{O^{2+}}, \mathrm{Ne^{2+}}, \mathrm{Ne^{4+}}, \mathrm{Ne^{6+}}, \mathrm{Ar^{6+}}$ at impact energies $E < 4$ keV amu^{-1} have been performed by means of absolute photon spectroscopy of the corresponding Li I ($\lambda = 670.8$ nm) radiation. The square brackets symbolize that neither primary nor secondary projectile states have been further specified. These measurements will be compared with our former experimental results for singly charged projectiles (Aumayr *et al* 1984a), as well as with large-scale atomic orbital close-coupling calculations (AO-CC) involving both bare $\mathrm{H^+}$, $\mathrm{He^{2+}}$ and $\mathrm{Be^{4+}}$ nuclei and incompletely ionized $\mathrm{C^{2+}}$ projectiles.

2. Experimental technique

We used a crossed-beams apparatus similar to the one described by Aumayr *et al* (1984a, b). Ions of interest were extracted from a 5 GHz ECR ion source (Leitner *et al* 1994), accelerated by up to 12 kV, focused by a magnetic quadrupole doublet, charge-to-mass separated by means of an analysing magnet and directed into the collision chamber. After passing the Li target atom beam the ions were collected in a Faraday cup. No attempt was made to determine the composition of the primary ion beam with respect to metastable state admixtures. Later in this paper it will be argued that the various TX cross sections are strongly influenced by competing SEC channels. For multicharged ion beams containing low-excited metastable admixtures it has been experimentally demonstrated that cross sections for SEC from Li(2s) do not differ substantially for ground state and related metastable state ions, respectively ('core conserving SEC', Brazuk *et al* 1984). Because of this experimentally proven situation no appreciable difference of the influence of SEC on TX by ground and related metastable state ions should also be expected. Additionally, in the present experimental investigations no dependence of measured TX cross sections on ECR ion source conditions has been found.

The Li atom beam was produced by effusion from a Knudsen cell inside a heated oven (Aumayr *et al* 1984a, b) surrounded by radiation shields. An aperture collimated the effusive beam which could be stopped by a mechanical shutter in order to account for photon signals from excitation of residual gas molecules. After passing the interaction region the Li atom beam was stopped by a water-cooled trap. Background pressure during measurements was typically 10^{-7} mbar. Careful alignment of the oven assured that the ion and atom beams intersected each other precisely in the viewing line of the light collection system. Single-collision conditions were assured by monitoring the fraction of charge-exchanged primary ions with and without the Li target beam.

Li I (670.8 nm) line radiation from the ion–atom interaction region was detected by a cooled EMI 9893 QB/100 photomultiplier equipped with a Schott type MA 7-0.5 interference filter. Polarization-related influences were avoided by viewing under the 'magic' angle of

54.7° with respect to the ion-beam axis. The observation length of the photon detection system was defined by slits to 6.5 mm along the ion-beam axis, in order to reduce background from excitation of residual gas molecules or scattered Li atoms.

The accumulation time for the photomultiplier counting signal was controlled by a data acquisition program which also provided for recording and integration of the primary ion-beam current up to a presettable charge, to minimize the influence of primary ion-beam fluctuations. Measuring cycles were performed with ion and/or Li atom beams on and/or off for proper background discrimination.

Relative values of the Li I emission cross sections were determined with respect to the reference impact energy of $10q$ keV, and stability of the Li target was checked by repeatedly taking data at this reference impact energy.

Absolute calibration of the resulting relative data was then obtained by comparing signals produced by ions of present interest to the signal produced by 10 keV proton impact excitation, making use of the absolute Li I emission cross sections for proton impact from Aumayr *et al* (1984a).

Statistical errors of our relative cross sections, which are mainly caused by counting statistics and Li target fluctuations, are typically around ±5% for ions in low charge states and up to ±15% for the highest ion charge states involved. In addition to these uncertainties, a quoted error of ±25% of the absolute reference cross section (Aumayr *et al* 1984a) has to be taken into account, leading to total errors in the range of ±25–30%.

Our measured Li I(2s ← 2p) emission cross sections differ from the related Li(2p ← 2s) excitation cross sections because of cascade contributions to the population of Li(2p) from higher excited Li(nl) levels ($n > 2$).

3. AO calculations

We applied the well known semiclassical impact-parameter formulation of the close-coupling (CC) method, assuming straight-line trajectories for the projectiles. This approach has already been described by Horvath *et al* (1996) (and references therein), which shall not be repeated here. Only details for the particularly chosen expansions and potentials will be given.

All chosen basis sets used in the present CC calculation are listed in table A1. This table has to be regarded just as a survey, and full information about the used basis set is available from the authors on request. Besides atomic orbitals (AO) on projectile and target, pseudostates (PS) on both centres are included in order to represent continuum states in the expansion. The latter are linear combinations of Slater-type orbitals (STOs, defined by charge z and n, l quantum numbers) with z values (not given in table A1) between the charge of the separated atoms and the united atom (quasimolecule) built up by the collision partners.

The interaction between the Li^+ core and the 'active' electron is described by an analytic model potential (Peach *et al* 1988). A potential with the same analytic structure as in the case of Li was chosen to describe the C II levels. Eigenvalues corresponding to this potential agree with experimental ones (Bashkin and Stoner 1975) within a few per cent, which is sufficient to model the SEC channels in AO calculations which were mainly optimized to produce accurate TX cross sections.

All presented AO calculations involve a considerable number of projectile centred states representing SEC. The importance of these SEC channels for the results of TX cross sections has already been discussed for He^{2+}–Li(2s) by Schweinzer *et al* (1994). In this theoretical study an amazing influence of the number of included SEC channels in an AO-

CC calculation on the TX process has been found for $E < 8$ keV amu^{-1}, but practically no influence for $E > 12$ keV amu^{-1}. In the latter impact energy range practically a pure one-centre expansion is sufficient to produce reliable TX cross sections. Between the two mentioned impact energy limits decoupling of TX from SEC channels occurs.

In order to compare experimental Li(2s $\leftarrow$ 2p) emission cross sections with results from AO-CC calculations, the most important cascade contributions had to be taken into account by using branching ratios given by Wiese *et al* (1966).

$$\sigma(2\mathrm{p} \leftarrow 2\mathrm{s}) = \boldsymbol{\sigma}(\mathbf{2p}) + \sigma(3\mathrm{s}) + \sigma(3\mathrm{d}) + \sigma(4\mathrm{f}) + 0.76\sigma(4\mathrm{p}) + 0.94\sigma(4\mathrm{d}) + 0.89\sigma(4\mathrm{s}). \tag{1}$$

The possibility of getting large cascade contributions to measured Li(2s $\leftarrow$ 2p) emission cross sections must be taken into account (cf equation (1)), because of the high branching ratios of decaying higher excited states which might also be populated in the collision process. This implies that also calculations of TX cross sections for these higher states are required to permit an accurate comparison between measured and theoretical results. Theoretical TX and Li(2s $\leftarrow$ 2p) emission cross sections resulting from AO27_32, AO51_64 and AO79_32 calculations are summarized in table A5.

4. Presentation of experimental results and comparison with calculated data

The projectile ions have been selected in line with our efforts to find scaling relations. In order to check characteristic dependences on Z and charge state q, various ions with different Z but the same charge state as well as ions of the same Z but in different charge states have been chosen.

For presentation, our experimental results for Li I emission in Z^{q+} + Li(2s) collisions were arranged following the same idea. Error bars do not include the uncertainty of the reference cross section used for calibration (cf above).

Quite surprising is the striking difference in TX cross sections for He^{2+} and the heavier doubly charged projectiles (figure 1). For the latter we found oscillations at $E \approx 1$ keV amu^{-1}, whereas data for He^{2+} merely show a weak kink at $E \approx 4$ keV amu^{-1}. This already indicates a clear dependence of TX cross section on the projectile species and its electronic structure.

While for C^{4+} an even more pronounced plateau structure appears at $2 \leqslant E \leqslant 4$ keV amu^{-1} (figure 2), no such structure has been observed for Ne^{4+}. Results for Ne^{6+} and Ar^{6+} (figure 3) show no significant structure of cross sections with the investigated impact energies.

Cross sections for C^{q+} and Ne^{q+} exhibit no clear trends concerning the charge state of the projectile (figure 4).

All data presented in figures 1–4 are also given in tables A2–A4.

We now compare our theoretical results for Li(2p $\leftarrow$ 2s) excitation in collisions with Z^{q+} ($q = 1, 2, 4$) projectiles to the experimental data presented above as well as data from other groups. Effects due to the electronic structure of the projectiles, however, could not be covered for all projectiles since our calculations mainly involve fully stripped ions.

As a general trend, agreement between experimental and theoretical results was found to decrease with increasing charge state of the projectile.

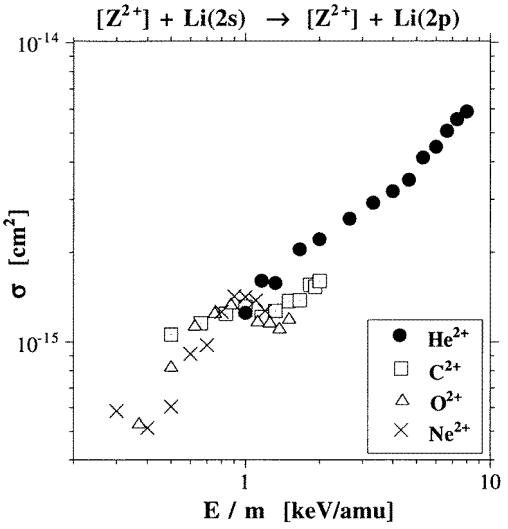

Figure 1. Measured Li I (670.8 nm) emission cross sections for impact of various doubly charged ions versus ion impact energy per atomic mass unit.

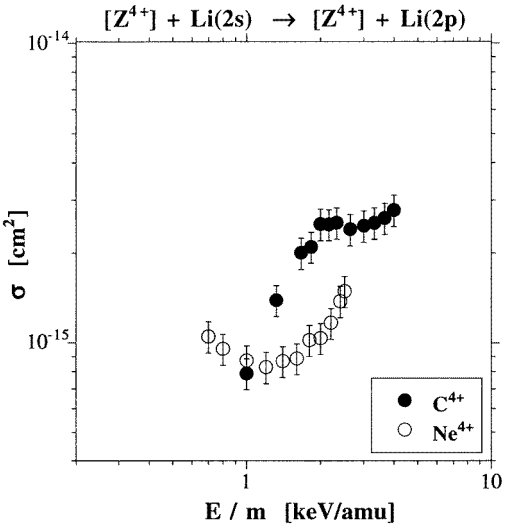

Figure 2. Measured Li I (670.8 nm) emission cross sections for impact of quadruply charged ions versus ion impact energy per atomic mass unit.

4.1. Singly charged projectiles

In the context of this work, we did not perform experimental investigations of impact excitation of Li(2s) by singly charged ions. Our theoretical results, however, are in excellent agreement with earlier experimental values (cf figure 5) from Aumayr *et al* (1984a, 1987). Convergence of AO-CC is demonstrated by comparison of AO27_36 and AO65_64 calculations for a reduced number of impact energies (cf figure 5). Cascade contributions

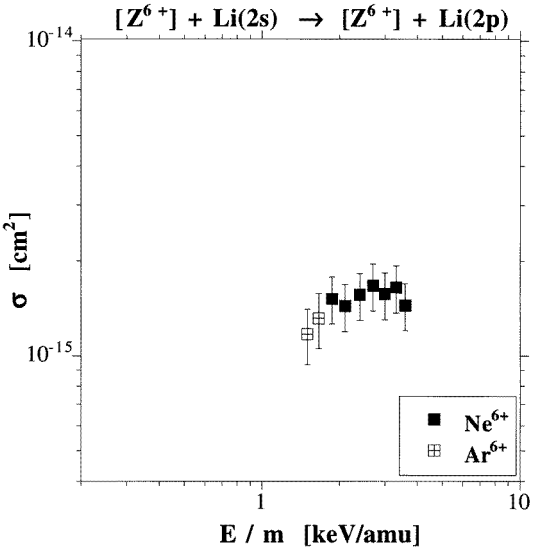

Figure 3. Measured Li I (670.8 nm) emission cross sections for impact of sextuply charged ions versus ion impact energy per atomic mass unit.

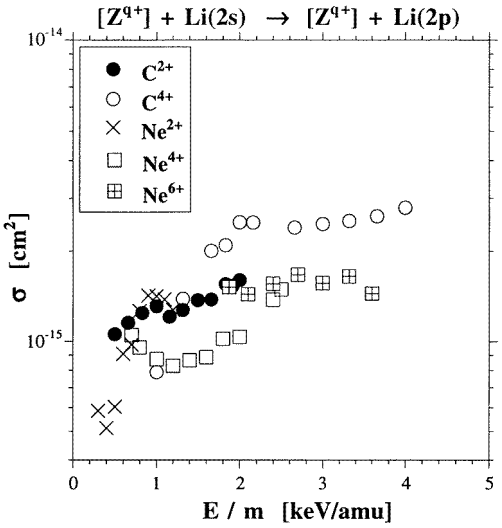

Figure 4. Measured Li I (670.8 nm) emission cross sections for impact of C^{q+} and Ne^{q+} ions versus ion impact energy per atomic mass unit.

to the emission cross sections increase from 3% at 5 keV amu^{-1} to 13% at 30 keV amu^{-1}.

Determination of the Li(2p $\leftarrow$ 2s) excitation cross section for impact of protons was performed by Aumayr *et al* (1984a) by estimating the Li(2p $\leftarrow$ 3*l*) cascade contributions to the Li I 670.8 nm emission from an AO calculation of Ermolaev (1984). For impact energies below $E = 8$ keV this calculation overestimates the Li(3*l* $\leftarrow$ 2s) TX cross sections considerably. Thus, the such derived Li(2p $\leftarrow$ 2s) excitation cross sections from Aumayr

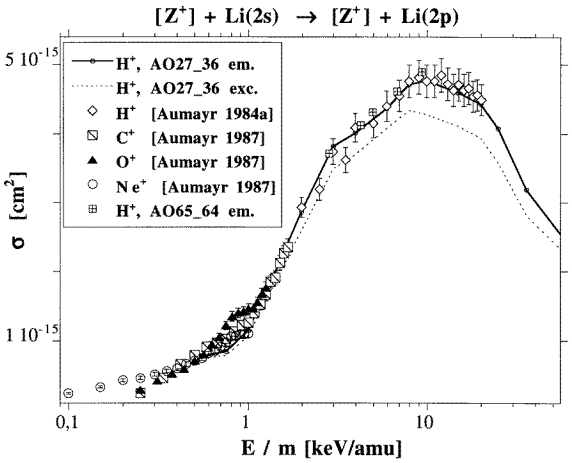

Figure 5. Measured (Aumayr *et al* 1984a, 1987) and calculated Li I$(2p \leftarrow 2s)$ emission cross sections plotted versus impact energy for various singly charged projectiles colliding with Li(2s). The theoretical Li$(2s \rightarrow 2p)$ excitation cross sections are also presented.

et al (1984a) for low impact energies were underestimated by up to 20% in comparison with our new theoretical results, which on the other hand agree almost perfectly with the measurements when emission cross sections are compared.

Measured emission cross sections for singly charged projectiles show no dependence on the number of core electrons (compare results for H^+, C^+, O^+ in figure 5), except at low impact energies $E \leqslant 1$ keV amu^{-1}. There, results for the heavier ion species deviate from each other as well as from the theoretical curve for protons, and data for O^+ and Ne^+ also indicate a small plateau structure in the TX cross section.

4.2. Doubly charged projectiles

Calculations have been performed for He^{2+} and C^{2+}. The agreement between experimental and AO-CC data for He^{2+} is very good. In the higher impact energy range, theory is about 5% above the measured values. Most probably the cascade contributions to the emission cross section are overestimated by our calculations. Convergence of AO calculations concerning the TX cross sections for the higher Li$(nl, n \geqslant 3)$ states has not been checked in this collision system, so far. Improvement of this situation would first require an increase in the number of SEC channels.

A plateau structure which is found experimentally for impact energies around 1–3 keV amu^{-1} for all projectiles (cf figure 6) except He^{2+}, is reproduced well by our AO-CC calculations for C^{2+}. The number of states on the projectile and target is the same for these two calculations. The calculations differ in the binding energy of final projectile states which can be populated by SEC. In the case of He^{2+} impact (SEC into l degenerated hydrogen-like states), only a few final states fit to favourable energy defects ΔE (Li(2s) ionization energy minus final binding energy of the active electron) for the SEC process. In the case of C^{2+} a larger number of final states with similar binding energies fit into the SEC 'reaction window' (Taulbjerg 1986). Since TX at these impact energies is in strong competition with the SEC process, details of the electronic structure of the projectile core and thus the situation of orbitals which might be populated leading to SEC or which

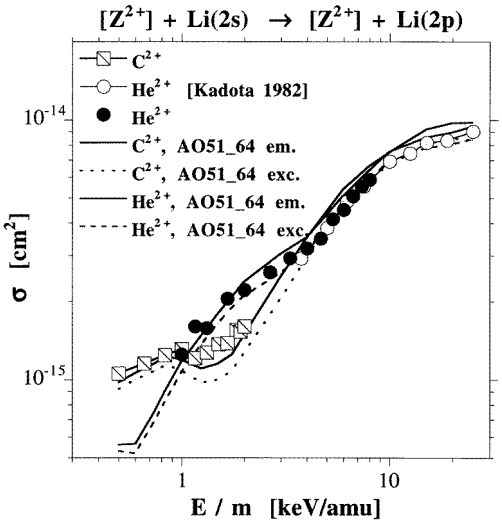

Figure 6. Measured and calculated Li I (670.8 nm) emission cross sections versus impact energy for impact of C^{2+} and He^{2+}. For comparison theoretical Li(2p) excitation cross sections are also plotted.

are just transiently populated during the collision, should influence the TX cross section considerably. In the higher impact energy range $E > 4$ keV amu^{-1}, however, differences between the two collision systems almost vanish, because the TX reaction channel becomes increasingly decoupled from the SEC channel (Horvath *et al* 1996).

The differences in TX cross sections when switching from He^{2+} to C^{2+} projectile persist if the number of states in AO-CC expansions is reduced to the most important ones (He^{2+}, C^{2+}: all $n = 3$ states, Li: 2s, 2p). This proves that these differences for the two projectile species are not due to different couplings involving many states. Therefore analysis of the potential curves for the quasimolecules (He^{2+}Li) and (C^{2+}Li), and a reduced calculation including only the most important couplings, could probably bring a still better understanding of this surprising result.

4.3. Quadruply charged projectiles

Several AO calculations for the fully stripped Be^{4+} ion have been performed with different basis sets. We compare three AO-CC calculations with different numbers of SEC channels and the same number of Li target states to demonstrate the importance of competition between SEC and TX at low impact energies (figure 7).

Whereas theoretical results for excitation into Li(2p) reach a high level of convergence, the convergence of cross sections for higher excited Li(nl) states ($n > 2$) is not satisfactory, even if the size of the basis set is already rather high. Therefore, no further attempt has been made to calculate emission cross sections for these collision systems.

Anyhow, a plateau structure can be seen clearly for the experimental as well as theoretical results.

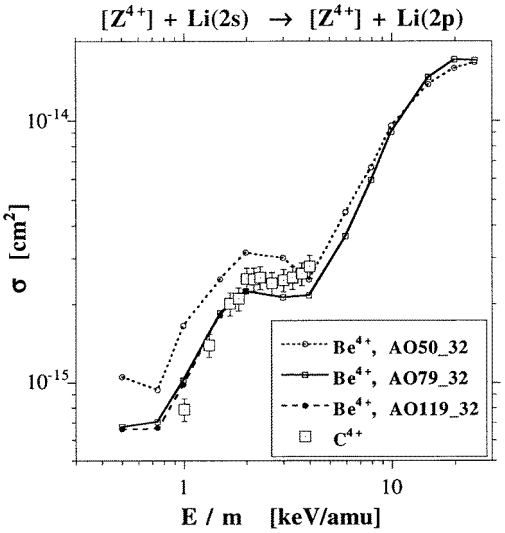

Figure 7. Measured Li I (670.8 nm) emission and calculated Li(2p ← 2s) excitation cross sections plotted versus impact energy for impact of quadruply charged ions.

5. Discussion of scaling with respect to q and comparison with TX of Na(3s)

A well established scaling σ/q versus E/q (Janev and Presnyakov 1980) with respect to q is appropriate for higher impact energies $E/q \geqslant 6$ keV amu^{-1} only, as can be clearly seen by comparing figures 8(*a*) and (*b*) (note the different scaling). The large differences in Li(2s ← 2p) TX cross section with varying projectile charge in the $E \geqslant 6$ keV amu^{-1} region (cf figure 8(*b*)) is transformed to one general cross section curve in the σ/q versus E/q plane for $E/q \geqslant 6$ keV amu^{-1} (cf figure 8(*a*)).

For higher impact energies, differences in TX cross sections are due only to different energy defects of the excitation process. Because of the higher excitation energy in the case of Na(3p ← 3s) in comparison with Li(2p ← 2s) TX cross sections for the latter are slightly larger than for Na.

Below collision energies of $E \approx 6$ keV amu^{-1} (cf figure 8(*b*)) no regular behaviour can be observed for TX cross sections in the various collision systems. In particular, the occurrence of a plateau structure and its energetic position depend strongly on the collision system. The striking result found for Na target atoms (Horvath *et al* 1996) that both the position of the plateau structure as well as the absolute cross section within the region of the plateau structure turned out to be almost independent of the projectile charge q (cf figure 8(*b*) and Horvath *et al* 1996), could not be confirmed for the same projectiles colliding with Li. The plateau structures in the TX cross sections appear at different impact energies for Li and Na, respectively (cf $C^{2+} + Li$ and $He^{2+} + Na$ results, figure 9). This comparison proves that TX cross sections in this impact energy range depend on individual features of the various collision systems. Therefore, an application of simple scaling relations resulting in a single general cross section curve seems not to be available.

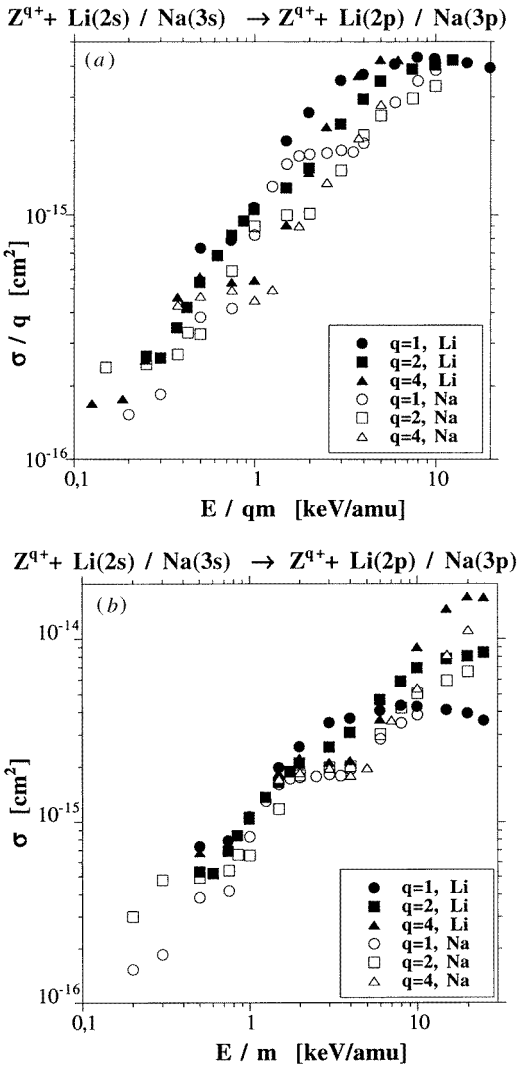

Figure 8. (*a*) Comparison of AO calculations for target excitation of Li and Na atoms by impact of Z^{q+} ions. (*b*) Comparison of AO calculations for target excitation of Li and Na atoms by impact of Z^{q+} ions.

6. Summary and conclusions

Experimental and calculated data for Li(2p ← 2s) excitation in collisions of Li(2s) atoms with slow ($v \leqslant 1$ au) singly and multiply charged ions have been presented and show the following general trends.

TX cross sections do not obey a general scaling relation in the low-energy regime with respect to the charge state of the projectile, but for reduced impact energies $E/q \geqslant$ 6 keV amu^{-1} the established TX scaling σ/q versus E/qm is verified. This 'threshold' energy E_{scal} for validity of the scaling relation depends most probably on the excitation energy for the TX process regarded.

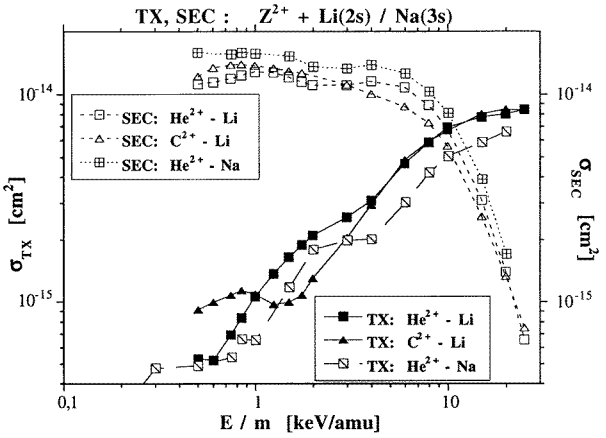

Figure 9. Comparison of TX and SEC cross sections for impact of He^{2+} and C^{2+} on Na and Li, respectively. TX cross sections are lower for Na, whereas SEC cross sections are lower for Li.

TX at lower impact energies is strongly influenced by the competing process of SEC. Coupling of SEC and TX channels causes some plateau structures in the TX cross sections. The binding energies of available final SEC projectile states relative to the initial and final states of the TX process seem to be decisive for the occurrence of the plateau structure and its position with respect to impact energy, while a detailed reason for this plateau structure is still missing.

A rough prediction whether 'core-effects' due to the projectile are influencing the TX cross section can be made by considering the ratio E/qE_{scal}. When this ratio exceeds unity no core effects have to be expected, simply because the SEC is completely decoupled from the TX process as already mentioned. However, as long as this ratio stays below unity, different TX cross sections might occur for projectiles of equal charge state but with different numbers of core electrons. In this region the modification of final SEC projectile states induced by the core electrons seems to be decisive for the observed differences in TX cross sections, e.g. rather similar TX cross sections are found for Be^{4+} and C^{4+} projectiles (cf figure 7), which considerably differ from the ones for Ne^{4+} projectiles (cf figure 2), as expected from a comparison of projectile cores $1s^2$ and $1s^22s^22p^2$ for C^{4+} and Ne^{4+}, respectively. Thus, closed-shell projectile core configurations are expected to have only small effects on the TX cross section in comparison with equally naked projectiles, even at much lower impact energies than E_{scal}.

Agreement between theory and experiment is excellent for singly charged projectiles, but becomes increasingly worse with increasing projectile charge. In the calculations convergence for TX to higher excited states—which would be important for cascade contributions to the Li I emission cross sections studied here—is hard to reach, since a huge number of SEC channels are needed in order to reach sufficient accuracy.

Acknowledgments

This work has been performed within the Association EURATOM-OEAW and was supported by Friedrich Schiedel-Stiftung für Energietechnik.

Appendix

Table A1. Basis sets used in CC calculations for TX and SEC in $Z^{q+} + \mathrm{Li}(2s)$ collisions. For distinction between AO and PS, all states on both centres are given for each CC calculation. Hydrogenic orbitals are used for the bound states of H I, He II, C II and Be IV. No specification of l means the full set of l quantum numbers for a given n. Linear combinations of STO are used as PS and for representation of AO Li I states. All calculations are specified by the number of states defined on the projectile (p) and the target (t) centre (i.e. AOp_t), respectively.

	Centre on projectile Z^{q+}		Centre on Li^+	
Calculation	AO states	PS states	AO states	PS states
H^+				
AO27_36	$n = 1, 2, 3$	17 STO $l \leqslant 3$	$n = 2, 3$	27 STO $l \leqslant 3$
AO65_64	$n = 1, 2, 3, 4$	45 STO $l \leqslant 4$	$n = 2, 3, 4$	45 STO $l \leqslant 4$
He^{2+}, C^{2+}				
AO51_64	$n = 1, 2, 3, 4$	31 STO $l \leqslant 4$	$n = 2, 3, 4$	45 STO $l \leqslant 4$
Be^{4+}				
AO50_32	$n = 1, 2, 3, 4, 5$	6h	$n = 2, 3$	23 STO $l \leqslant 2$
AO79_32	$n = 1, 2, 3, 4, 5, 6, 7$; $\lvert m\rvert \leqslant 4$	—	$n = 2, 3$	23 STO $l \leqslant 2$
AO119_32	$n = 1, 2, 3, 4, 5, 6, 7, 8$	—	$n = 2, 3$	23 STO $l \leqslant 2$

Table A2. Measured Li I($2s \leftarrow 2p$) emission cross sections for impact of various doubly charged ions.

Z^{q+}	E/m (keV amu^{-1})	σ (cm^2)	$\Delta\sigma/\sigma$ (±%) relative	$\Delta\sigma/\sigma$ (±%) absolute
He^{2+}	1.00	1.25e−15	3.7	25.5
	1.16	1.60e−15	1.5	25.5
	1.32	1.58e−15	2.3	25.5
	1.66	2.05e−15	4.0	25.5
	2.00	2.21e−15	2.0	25.5
	2.66	2.59e−15	1.8	25.5
	3.32	2.93e−15	1.4	25.5
	4.00	3.19e−15	1.9	25.5
	4.66	3.48e−15	2.1	25.5
	5.32	4.14e−15	2.8	25.5
	6.00	4.50e−15	2.2	25.5
	6.66	5.08e−15	2.4	25.5
	7.32	5.54e−15	2.2	25.5
	8.00	5.88e−15	1.5	25.5
C^{2+}	0.66	1.15e−15	3.9	25.5
	0.83	1.24e−15	1.8	25.5
	1.00	1.31e−15	5.7	25.5
	1.16	1.21e−15	2.7	25.5
	1.32	1.27e−15	4.3	25.5
	1.50	1.37e−15	6.8	26.0
	1.66	1.38e−15	2.0	25.5
	1.83	1.56e−15	3.8	25.5

Table A2. (Continued)

Z^{q+}	E/m (keV amu^{-1})	σ (cm^2)	$\Delta\sigma/\sigma$ (±%) relative	$\Delta\sigma/\sigma$ (±%) absolute
	1.91	1.53e−15	8.5	26.2
	2.00	1.60e−15	7.8	26.2
O^{2+}	0.37	5.35e−16	8.7	26.5
	0.50	8.30e−16	4.8	25.6
	0.63	1.14e−15	2.9	25.5
	0.75	1.26e−15	3.6	25.5
	0.87	1.35e−15	3.1	25.5
	1.00	1.37e−15	3.5	25.5
	1.12	1.18e−15	1.8	25.5
	1.25	1.17e−15	3.0	25.5
	1.37	1.12e−15	1.3	25.5
	1.50	1.21e−15	9.0	26.7
Ne^{2+}	0.30	5.86e−16	8.7	26.5
	0.40	5.13e−16	4.8	25.6
	0.50	6.05e−16	2.9	25.5
	0.60	9.10e−16	3.6	25.5
	0.70	9.75e−16	3.1	25.5
	0.80	1.26e−15	3.5	25.5
	0.90	1.42e−15	1.8	25.5
	1.00	1.42e−15	3.0	25.5
	1.10	1.12e−15	1.3	25.5
	1.20	1.21e−15	9.0	26.7

Table A3. Measured Li I(2s ← 2p) emission cross sections for impact of quadruply charged ions.

Z^{q+}	E/m (keV amu^{-1})	σ (cm^2)	$\Delta\sigma/\sigma$ (±%) relative	$\Delta\sigma/\sigma$ (±%) absolute
C^{4+}	1.00	7.88e−16	14.3	29.4
	1.32	1.38e−15	10.0	27.1
	1.66	2.00e−15	12.6	28.1
	1.83	2.09e−15	8.9	26.6
	2.00	2.49e−15	9.7	27.1
	2.16	2.49e−15	8.9	26.6
	2.32	2.52e−15	9.1	27.0
	2.64	2.40e−15	8.0	26.2
	3.00	2.46e−15	8.5	26.4
	3.32	2.52e−15	8.5	26.4
	3.66	2.62e−15	6.9	26.0
	4.00	2.78e−15	11.3	27.3
Ne^{4+}	0.70	1.05e−15	10.4	26.9
	0.80	9.53e−16	8.6	26.4
	1.00	8.71e−16	7.1	26.0
	1.20	8.27e−16	8.3	26.3
	1.40	8.66e−16	7.9	26.2
	1.60	8.85e−16	7.8	26.2
	1.80	1.02e−15	8.2	26.3

Table A3. (Continued)

Z^{q+}	E/m (keV amu^{-1})	σ (cm^2)	$\Delta\sigma/\sigma$ (±%) relative	$\Delta\sigma/\sigma$ (±%) absolute
	2.00	1.03e−15	6.7	25.8
	2.20	1.16e−15	7.1	26.0
	2.40	1.38e−15	7.4	26.1
	2.50	1.49e−15	6.9	25.9

Table A4. Measured Li I(2s ← 2p) emission cross sections for impact of sextuply charged ions.

Z^{q+}	E/m (keV amu^{-1})	σ (cm^2)	$\Delta\sigma/\sigma$ (±%) relative	$\Delta\sigma/\sigma$ (±%) absolute
Ne^{6+}	1.87	1.51e−15	7.1	26.0
	2.10	1.43e−15	6.8	25.9
	2.40	1.56e−15	6.9	25.9
	2.70	1.66e−15	6.2	25.8
	3.00	1.56e−15	5.6	25.6
	3.32	1.64e−15	13.2	28.3
	3.60	1.44e−15	8.1	26.3
Ar^{6+}	1.50	1.17e−15	12.0	27.8
	1.66	1.31e−15	20.6	32.3

Table A5. Calculated Li I(2s ← 2p) excitation (TX) and Li I(2s ← 2p) emission (EM) cross sections (units: 10^{-16} cm^2) in collisions of H^+, He^{2+}, C^{2+} and Be^{4+} with Li(2s). Results originate from AO-CC calculations AO27_36, AO51_64 and AO79_32 for projectiles H^+, (He^{2+}, C^{2+}) and Be^{4+}, respectively (see table A1).

	H^+		He^{2+}		C^{2+}		Be^{4+}
E (keV amu^{-1})	TX	EM	TX	EM	TX	EM	TX
0.5	7.3	7.6	5.3	5.5	9.2	9.7	6.8
0.75	7.9	8.4	6.9	7.4	10.8	11.6	7.1
1.0	10.7	11.5	10.6	11.3	10.9	12.0	10.2
1.5	19.9	21.5	16.5	17.4	10.0	11.5	18.5
2.0	25.9	28.6	21.0	22.8	13.0	15.9	22.4
3.0	34.9	38.1	25.7	29.5	20.5	24.8	21.2
4.0	37.0	40.1	30.9	34.3	29.5	35.0	21.6
6.0	40.8	43.7	46.6	49.6	48.6	53.9	36.4
8.0	43.4	47.1	58.8	62.2	59.6	66.2	59.3
10.0	42.8	47.7	69.5	73.4	67.0	75.0	90.6
15.0	41.1	45.9	77.9	82.3	80.7	91.9	146.0
20.0	39.4	44.3	80.7	86.2	84.9	97.2	170.0
25.0	35.8	40.7	84.5	91.7	83.7	97.9	169.0

References

Aumayr F, Fehringer M and Winter H P 1984a *J. Phys. B: At. Mol. Phys.* **17** 4185–99

——1984b *J. Phys. B: At. Mol. Phys.* **17** 4201–11

Aumayr F, Lakits G and Winter H P 1987 *Z. Phys.* D **6** 145–53

Aumayr F, Schorn R P, Pöckl M, Schweinzer J, Wolfrum E, McCormick K, Hintz E and Winter H P 1992 *J. Nucl. Mater.* **196–198** 928–32

Bashkin S and Stoner J O 1975 *Atomic Energy Levels and Grotrian Diagrams* vol 1 (Amsterdam: North-Holland)

Brazuk A, Dijkkamp D, Drentje A G, de Heer F J and Winter H P 1984 *J. Phys. B: At. Mol. Phys.* **17** 2489
Ermolaev A M 1984 *J. Phys. B: At. Mol. Phys.* **17** 1069
Ermolaev A M, Hewitt R N, Shingal R and McDowell M R C 1987 *J. Phys. B: At. Mol. Phys.* **20** 4507
Horvath G, Schweinzer J, Winter H P and Aumayr F 1996 *Phys. Rev.* A **54** 3022–8
Kadota K, Dijkkamp D, van der Woude R L, Yan P G and de Heer F J 1982 *J. Phys. B: At. Mol. Phys.* **15** 3297
Janev R K 1996 *Phys. Rev.* A **53** 219–24
Janev R K and Presnyakov L P 1980 *J. Phys. B: At. Mol. Phys.* **13** 4233
Leitner M, Wutte D, Brandstötter J, Aumayr F and Winter H P 1994 *Rev. Sci. Instrum.* **65** 1091–3
Peach G, Saraph H E and Seaton M J 1998 *J. Phys. B: At. Mol. Opt. Phys.* **21** 3669–83
Schorn R P, Hintz E, Rusbüldt D, Aumayr F, Schneider M, Unterreiter E and Winter H P 1991 *Appl. Phys.* B **52** 71–8
Schorn R P, Wolfrum E, Aumayr F, Hintz E, Rusbüldt D and Winter H P 1992 *Nucl. Fusion* **32** 351–9
Schweinzer J, Wolfrum E, Aumayr F, Pöckl M, Winter H P, Schorn R P, Hintz E and Unterreiter A 1992 *Plasma Phys. Control. Fusion* **34** 1173–83
Schweinzer J, Wutte D and Winter H P 1994 *J. Phys. B: At. Mol. Opt. Phys.* **27** 137–53
Taulbjerg K 1986 *J. Phys. B: At. Mol. Phys.* **19** L367
Wiese W L, Smith M W and Glennon B M 1966 *Atomic Transition Probabilities (NSRDS-NBS 4)* vol 1 (Washington, DC: US Govt Printing Office)
Wolfrum E, Aumayr F, Wutte D, Winter H P, Hintz E, Rusbüldt D and Schorn R P 1993 *Rev. Sci. Instrum.* **64** 2285–92
Wutte D, Janev R K, Aumayr F, Schneider M, Schweinzer J, Smith J J and Winter H P 1997 *At. Nucl. Data Tables* **65** 155–80